"Mechanistic insights into the formation of N_2O and N_2 in NO reduction by NH_3 over a polycrystalline platinum catalyst"

Vita A. Kondratenko, Manfred Baerns

Mechanistic insights into the formation of N_2O and N_2 in NO reduction by NH_3 over a polycrystalline platinum catalyst

Vita A. Kondratenko [*], Manfred Baerns

Leibniz-Institut für Katalyse e.V. an der Universität Rostock, Außenstelle Berlin, Richard-Willstaetter-Str. 12, D-12489 Berlin, Germany

Available online 30 June 2006

Abstract

The reaction pathways of N_2 and N_2O formation in the direct decomposition and reduction of NO by NH_3 were investigated over a polycrystalline Pt catalyst between 323 and 973 K by transient experiments using the temporal analysis of products (TAP-2) reactor. The interaction between nitric oxide and ammonia was studied in the sequential pulse mode applying ^{15}NO. Differently labelled nitrogen and nitrous oxide molecules were detected. In both, direct NO decomposition and NH_3–NO interaction, N_2O formation was most marked between 573 and 673 K, whereas N_2 formation dominated at higher temperatures. An unusual interruption of nitrogen formation in the ^{15}NO pulse at 473 K was caused by an inhibiting effect of adsorbed NO species. The detailed analysis of the product distribution at this temperature clearly indicates different reaction pathways leading to the product formation. Nitrogen formation occurs via recombination of nitrogen atoms formed by dissociation of nitric oxide or/and complete dehydrogenation of ammonia. N_2O is formed via recombination of adsorbed NO molecules. Additionally, both products are formed via interactions between adsorbed ammonia fragments and nitric oxide.
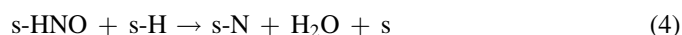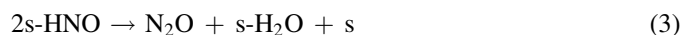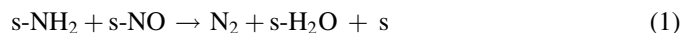© 2006 Elsevier B.V. All rights reserved.

Keywords: Mechanism; NO decomposition; NO reduction by NH_3; N_2O formation; ^{15}NO; Pt gauze; Transient experiments; TAP reactor

1. Introduction

The catalytic reduction of nitrogen oxides emissions for environmental protection has been a subject of numerous studies [1]. NO emission from nitric acid plants and stationary power stations is controlled by selective catalytic reduction (SCR) using ammonia or urea. Although metal-oxide catalysts are mostly applied, Pt-based catalysts are also of interest due to their high efficiency in the SCR process under sulphur-free conditions [2]. Moreover, the interaction of NO and NH_3 over Pt catalysts reveals rate oscillations, which gave rise to various detailed mechanistic studies [3–7] aimed at the understanding of the oscillatory behaviour. Besides, the NO–NH_3 interactions play a significant role in side product formation (N_2O and N_2) in the high-temperature ammonia oxidation to nitric oxide [8].

Various mechanistic studies of the interactions between NO and NH_3 on Pt-based catalysts [3–7,9–12] were performed in a broad range of pressures extending from UHV (10^{-7} to 10^{-5} Pa) [5–7,13] over mediate pressures of $10–10^2$ Pa [3,10]
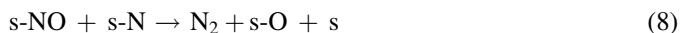
to ambient pressure [11,12]. The main reaction products were nitrogen and water. N_2O formation was only sporadically observed and discussed. The most informative insights into N_2 and N_2O formation were derived using isotopically labelled molecules (^{15}NO [6] and $^{15}NH_3$ [7,8,14]). The suggested concepts differ in the reaction pathways of product formation. Earlier mechanisms [3,9,10,14] consider the dissociation of ammonia to NH_2 and hydrogen atoms, which in turn react with adsorbed NO yielding HNO species. HNO and NH_2 species participate in the reaction pathways leading to N_2 and N_2O (Eqs. (1)–(5)). Although some indications for HNO species were obtained by EELS studies [15], their existence is still controversial:

$$s\text{-}NH_2 + s\text{-}NO \rightarrow N_2 + s\text{-}H_2O + s \tag{1}$$

$$s\text{-}NH_2 + s\text{-}NO \rightarrow N_2O + 2s\text{-}H \tag{2}$$

$$2s\text{-}HNO \rightarrow N_2O + s\text{-}H_2O + s \tag{3}$$

$$s\text{-}HNO + s\text{-}H \rightarrow s\text{-}N + H_2O + s \tag{4}$$

$$2s\text{-}N \rightarrow N_2 + 2s \tag{5}$$

* Corresponding author. Tel.: +49 30 63924414; fax: +49 30 63924454.
E-mail address: viko@aca-berlin.de (V.A. Kondratenko).

Later concepts [6,7] are based on a more general approach excluding the participation of HNO or NH$_2$ species. Nitrogen atoms are considered as a key intermediate in N$_2$ [6,7] and N$_2$O [7] formation (Eqs. (6)–(8)):

$$2s\text{-}N \rightarrow N_2 + 2s \qquad (6)$$

$$s\text{-}NO + s\text{-}N \rightarrow N_2O + 2s \qquad (7)$$

$$s\text{-}NO + s\text{-}N \rightarrow N_2 + s\text{-}O + s \qquad (8)$$

However, these concepts ignore the experimental observations that adsorbed ammonia fragments dominate on the Pt surface at low temperatures under oxidative conditions [16–18]. Therefore, further mechanistic examinations of the interactions between NO and NH$_3$ are needed. The present study was aimed at detailed understanding of reaction pathways leading to N$_2$ and N$_2$O in the NH$_3$–NO interaction over an industrially relevant knitted Pt gauze by means of transient experiments with isotopic tracers. NO decomposition, which also yields N$_2$ and N$_2$O over Pt catalysts [19–21], was taken into consideration in order to estimate its contribution to the overall product formation in NO reduction by NH$_3$. The transient experiments were performed in the temperature range from 323 to 973 K using the TAP-2 reactor. This technique enables the study of primary heterogeneous reaction steps due to the suppression of any possible gas-phase interactions. Due to the small amount of pulsed molecules, highly exothermic NH$_3$–NO reaction can be studied under isothermal conditions as it was earlier shown for ammonia oxidation [22].

2. Experimental

Knitted Pt gauze (Multinit® type 4, Degussa) made of polycrystalline Pt wire was used as a catalyst. The geometric surface area (0.002(4) m^2 g^{-1}) of the catalyst coincides well with the BET surface area (0.002(3) m^2 g^{-1}), determined by low-temperature adsorption of Kr, which was used because of the low surface area of the catalyst.

The TAP reactor system has been described in detail elsewhere [23,24]. A single piece of the catalytic gauze (ca. 120 mg) was placed between two layers of inert quartz particles (sieve fraction 250–350 μm) in the isothermal zone of a quartz-made micro reactor (i.d. = 0.006 m, L = 0.04 m). Before pulse experiments the gauze was pre-treated in a flow of O$_2$ (30 ml/min) at 1073 K for 1 h at atmospheric pressure to remove carbon deposits from the catalyst surface. For studying direct NO decomposition, the Pt gauze was treated in a flow of hydrogen (10 ml/min) at 873 K for 4 h at atmospheric pressure. After pre-treatment, the reactor was evacuated and the catalyst was exposed to vacuum conditions (10^{-5} Pa). During a single pulse the pressure in the catalyst zone increased to ca. 10 Pa.

Additionally, after NO pulsing at a specified reaction temperature the catalyst was treated by hydrogen pulsing (ca. 10^{16} molecules/pulse) in order to remove oxygen species formed from NO (Section 3.1). H$_2$ was pulsed over the gauze until no water signal was anymore observed at the reactor outlet. For experiments below 873 K this pulse treatment was

performed at 873 K, while for experiments above this temperature, the H$_2$-pulse treatment was carried out at the same temperature.

Transient experiments were performed using ^{14}NO/Ne = 1:1, ^{15}NO/Ne = 1:1 and ^{14}NH$_3$/Ne = 1:1 mixtures in the temperature range between 323 and 973 with 100 K intervals. The time interval between the NH$_3$ and ^{15}NO pulses was 0.2 s. The pulse size was kept for all experiments in the range of 5 × 10^{14} to 9 × 10^{14} molecules enabling operation in the Knudsen diffusion regime.

Ne (99.998%), Xe (99.99%), ^{15}NO (99.5%), ^{14}NH$_3$ (99.98 wt.%) were used as delivered. Isotopically labelled nitric oxide was purchased from ISOTEC. The following atomic mass units (AMUs) were used for mass-spectroscopic identification of different compounds: 44, 30, 28 (N$_2$O), 32 (O$_2$), 30 (NO), 28 (N$_2$), 18 (H$_2$O), 15 (NH$_3$), 2 (H$_2$), 20 (Ne) and 132 (Xe). In experiments with ^{15}NO, transient responses were additionally recorded at the AMUs: 46, 31, 30 (^{15}N$_2$O), 45, 31, 30, 29 (^{15}N^{14}NO), 31 (^{15}NO), 30 (^{15}N$_2$), 29 (^{15}N^{14}N).

3. Results

3.1. Decomposition of NO over platinum gauze

During NO pulsing over hydrogen-treated Pt gauze N$_2$ and N$_2$O were the only reaction products in the temperature range from 323 to 973 K. No O$_2$ was observed in the gas phase over the whole temperature range. However, the activity of hydrogen-treated Pt was not stable; the amount of decomposed NO as well as the amount of products decreased with the number of NO pulses as exemplified in Fig. 1 for 573 K. This decrease is more pronounced for N$_2$O than for N$_2$. The self inhibition of NO decomposition is discussed in Section 4.1.

The distribution of N$_2$O and N$_2$ formed from NO changes with temperature. The temperature dependence of the molar fractions of NO, N$_2$O and N$_2$, which correspond to the initial activity of Pt, is shown in Fig. 2. N$_2$O formation prevails at low
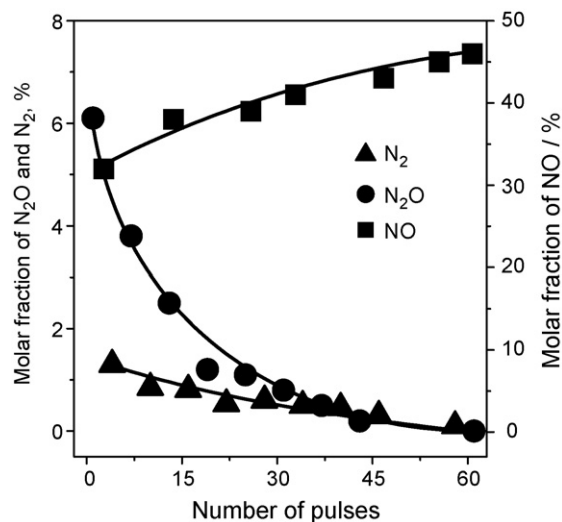

Fig. 1. Molar fractions of NO (■), N$_2$ (▲) and N$_2$O (●) as a function of number of NO pulses over hydrogen-treated Pt gauze at 573 K.
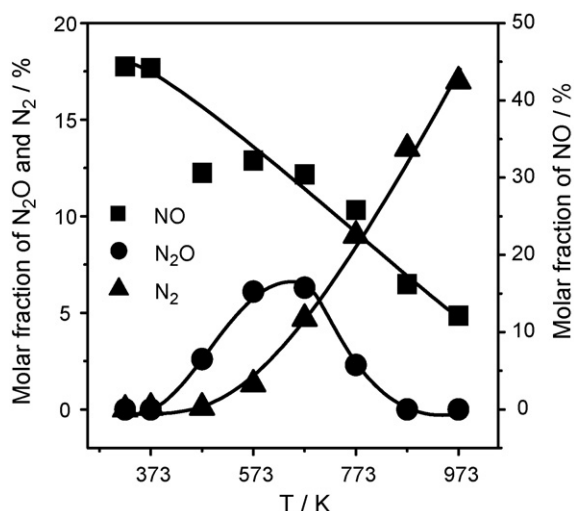
Fig. 2. Molar fractions of NO, N_2 and N_2O as a function of temperature when an NO/Ne mixture was pulsed over hydrogen-treated Pt gauze.

temperatures. Its production decreases after passing through a maximum between 573 and 673 K. N_2 becomes the main product at temperatures above 673 K. Some loss of NO as derived from a balance of the gas phase, especially marked at low temperatures, was explained by partially reversible NO adsorption. The type of NO interaction with Pt was determined by analysing of the transient responses of NO and Ne according to the method suggested by Gleaves et al. [24]. The responses of NO and Ne were transformed into a dimensionless form taking into account the effective diffusion coefficients, the amount of pulsed gases and the geometric dimensions of the micro reactor. The comparison between the modified responses of NO and Ne (Fig. 3), shows a typical "finger tip" for a reversible adsorption, i.e. the modified response of NO crosses that of Ne [24]. Formation of some irreversibly adsorbed NO species, which explains the loss of NO, can be expected over polycrystalline Pt below 650 K [25].
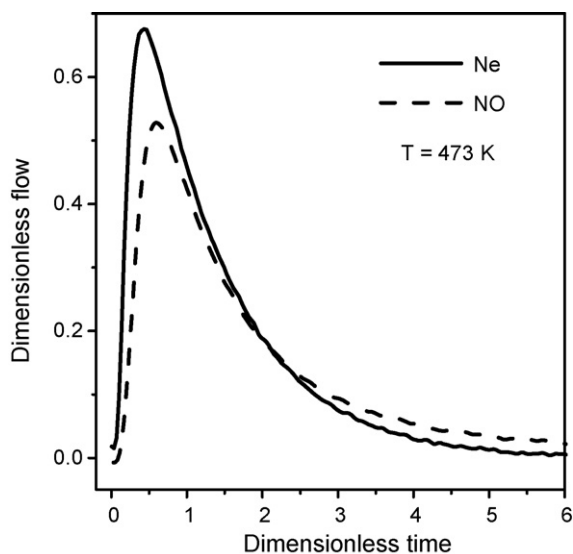
3.2. Reduction of nitric oxide by ammonia

For detailed mechanistic insights into the catalytic reduction of NO by NH_3 yielding N_2O and N_2, this reaction was comprehensively studied by sequential pulsing of $^{14}NH_3$ and ^{15}NO with a time delay of 0.2 s between pulses. Using of labelled nitric oxide in these experiments enables to identify different reaction pathways of product formation based on the distribution of labelled nitrogen atoms in the product molecules. The experimental results are presented below starting with the description of product formation in the $^{14}NH_3$ pulse followed by that in the ^{15}NO pulse.

$^{14}N_2$, H_2O and H_2 were the only reaction products in the $^{14}NH_3$ pulse. The temperature dependence of their formation is shown in Fig. 4. The formation of these products started above 473 K. The amount of formed H_2O achieved a maximum at 573 K. A further temperature increase led to a decrease of the amount of H_2O; it increased, however, again after passing through a minimum between 773 and 873 K. The formation of $^{14}N_2$ and H_2 increased with temperature in accordance with an increased degree of NH_3 decomposition over oxygen-treated Pt gauze as reported by us previously [26]. The increase in the amount of $^{14}N_2$ in the $^{14}NH_3$ pulse means that the amount of $^{14}NH_x$ species available for the reaction in the subsequent ^{15}NO pulse decreases, respectively.

In the subsequent ^{15}NO pulse, three nitrogen isotopes ($^{15}N_2$, $^{15}N^{14}N$ and $^{14}N_2$), as well as $^{15}N_2O$ and $^{15}N^{14}NO$ were observed besides H_2O. Traces of $^{14}N_2O$ were detected at 573 K only. The temperature dependence of the formation of differently labelled nitrogen and nitrous oxide molecules is shown in Figs. 5 and 6, respectively. $^{14}N_2$, formally formed from non-labelled $^{14}NH_3$ from preceding pulse, is the minor product in the ^{15}NO pulse over the whole temperature range. Its amount increases with temperature up to 573 K and decreases above this temperature. The formation of $^{15}N^{14}N$ and $^{15}N_2$ also passes through maxima at
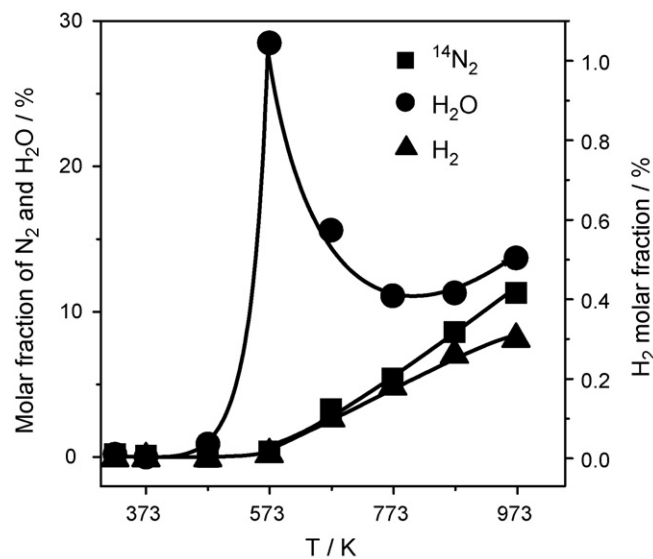

Fig. 3. Comparison between transient responses of NO and Ne treated according to the method suggested by Gleaves et al. [24].

Fig. 4. Molar fractions of $^{14}N_2$, H_2 and H_2O formed in the $^{14}NH_3$ pulse as a function of temperature when $^{14}NH_3$ and ^{15}NO were sequentially pulsed with time interval of 0.2 s.
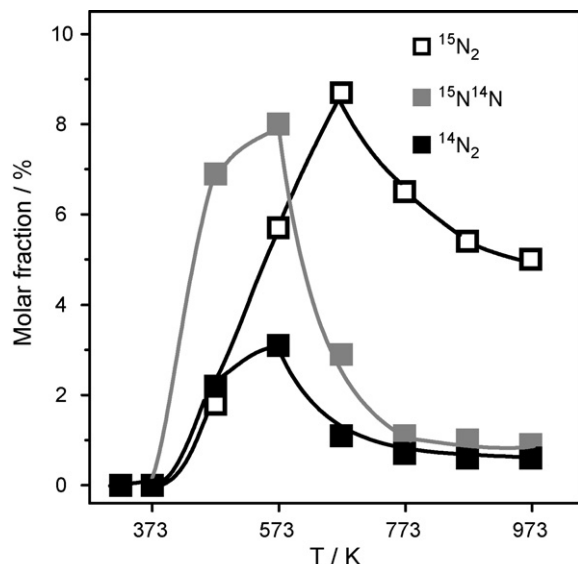
Fig. 5. Molar fractions of $^{15}N_2$, $^{15}N^{14}N$ and $^{14}N_2$ formed in the ^{15}NO pulse as a function of temperature when NH_3 and ^{15}NO were sequentially pulsed with time interval of 0.2 s.

Fig. 7. Transient responses of $^{15}N_2$, $^{15}N^{14}N$, $^{14}N_2$ and H_2O formed in the ^{15}NO pulse when $^{14}NH_3$ and ^{15}NO were sequentially pulsed with time interval of 0.2 s at 473 K.

573 and 673 K, respectively. $^{15}N^{14}N$ is preferentially formed in the temperature range of 473–573 K, whereas $^{15}N_2$ is the main product at higher temperatures. The decrease of the total nitrogen formation at elevated temperatures correlates with earlier observations [6,9,10]. This temperature effect has been explained by the temperature-induced changes of the distribution of reactive surface species on the catalyst surface [9]. Mechanistic aspects of the formation of various nitrogen isotopes are discussed in Section 4.3.

From a mechanistic point of view, the experimental data, obtained at 473 K are most interesting due to the observed interruption, i.e. temporary decrease to 0, in the formation of
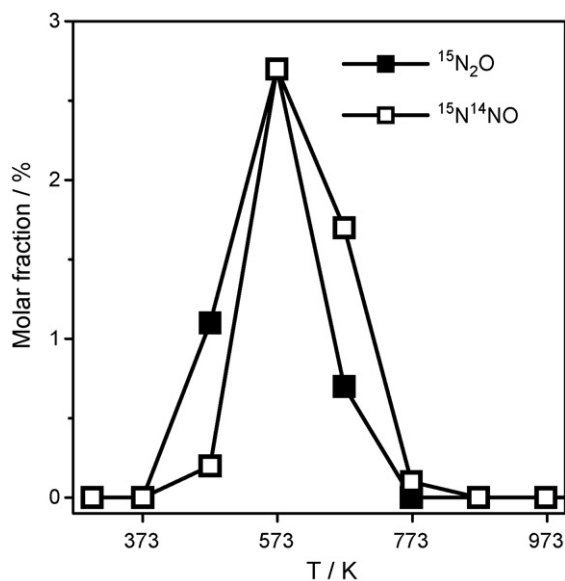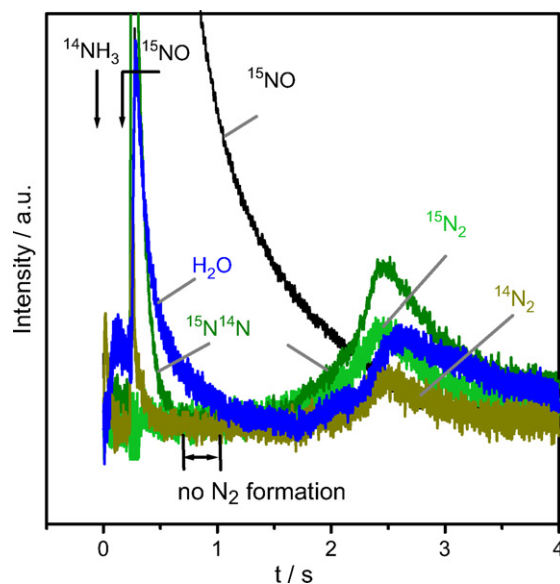
nitrogen and water upon entering of ^{15}NO in the micro reactor (Fig. 7). These products are formed in the ^{15}NO pulse between 0.2 and 0.7 s as well as between 1 and 4 s. Between 0.2 and 0.7 s $^{15}N^{14}N$ was the main product. In this time interval also a very small amount of $^{14}N_2$ was detected. The preferential formation of $^{15}N^{14}N$ ($n_{15_{N_2}} : n_{15_{N^{14}N}} : n_{14_{N_2}} = 0 : 2.4 : 0.6$) between 0.2 and 0.7 s (Fig. 7) indicates that there is a specific reaction pathway leading to this product only.

The second increase of $^{15}N^{14}N$ and $^{14}N_2$ formation between 1 and 4 s is accompanied by simultaneous appearance of $^{15}N_2$ in the gas phase. The distribution of differently labelled N_2 ($n_{15_{N_2}} : n_{15_{N^{14}N}} : n_{14_{N_2}} = 1.9 : 4.4 : 1.5$), formed between 1

Fig. 6. Molar fractions of $^{15}N_2O$ and $^{15}N^{14}NO$ formed in the ^{15}NO pulse as a function of temperature when $^{14}NH_3$ and ^{15}NO were sequentially pulsed with time interval of 0.2 s.
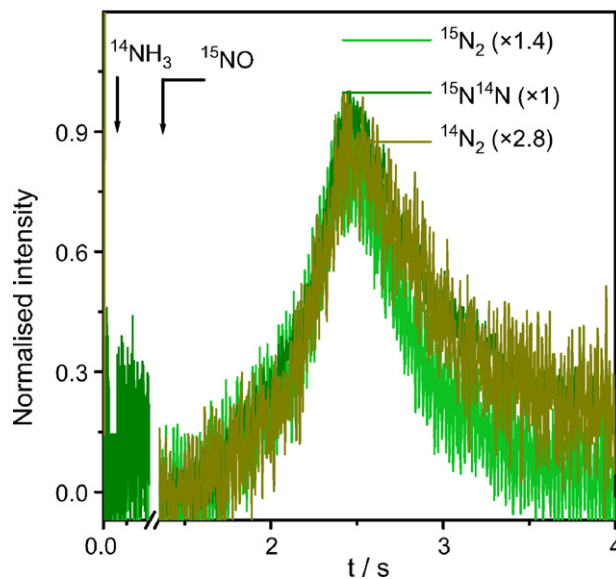

Fig. 8. Normalised responses of $^{15}N_2$, $^{15}N^{14}N$ and $^{14}N_2$ formed in the ^{15}NO pulse when $^{14}NH_3$ and ^{15}NO were sequentially pulsed with time interval of 0.2 s at 473 K.
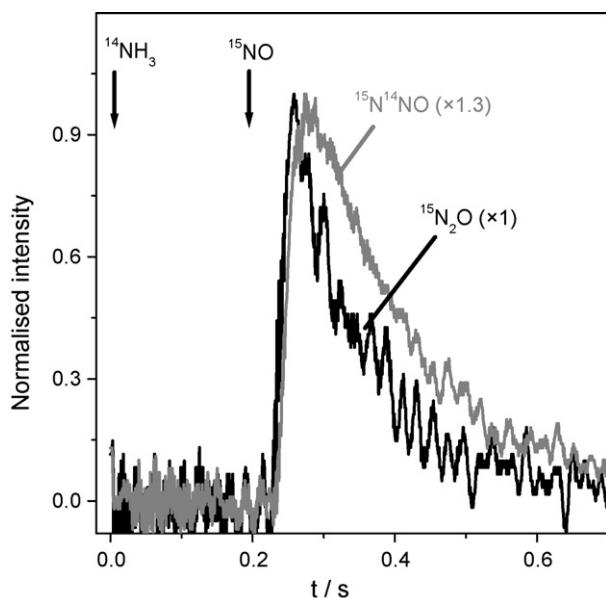
Fig. 9. Normalised responses of $^{15}N_2O$ and $^{15}N^{14}NO$ (×1.3) formed in the ^{15}NO pulse when NH_3 and ^{15}NO were sequentially pulsed with time interval of 0.2 s at 473 K.

and 4 s indicates, that N_2 forms via a process, which involves all types of nitrogen atoms. This assumption is supported by an analysis of the temporal appearance of these nitrogen isotopes at the reactor outlet. Fig. 8 compares the shapes of the normalised transient responses of $^{15}N_2$, $^{15}N^{14}N$ and $^{14}N_2$ between 1 and 4 s. It is clear that they are nearly similar. Such similarity can be explained by the likeness of the reaction pathways, which lead to the formation of differently labelled nitrogen molecules in this time interval.

In contrast to nitrogen formation, differently labelled N_2O molecules ($^{15}N_2O$ and $^{15}N^{14}NO$) are formed in the ^{15}NO pulses between 0.2 and 0.7 s only. The transient responses of $^{15}N_2O$ and $^{15}N^{14}NO$ differ in their shape and order of appearance (Fig. 9). The changes of molar fractions of $^{15}N_2O$ and $^{15}N^{14}NO$ with temperature are shown in Fig. 6. Similar to the temperature dependence of N_2O formation in the NO pulse experiments in Fig. 2, the formation of nitrous oxide passes through a maximum at 573 K in sequential pulsing of NH_3 and ^{15}NO. The decrease of the N_2O formation with temperature can be explained by increasing contribution of N_2O decomposition as well as by decreasing formation of N_2O due to enhanced NO desorption.

4. Discussion

4.1. NO decomposition

Hydrogen-treated Pt surface decomposes NO yielding N_2 and N_2O without any reducing agent. However, the activity of Pt towards product formation in NO decomposition decreases with an increase in the number of NO pulses (Fig. 1). Since no gas-phase oxygen was detected in these experiments, the decrease of Pt activity is attributed to the inhibiting effect of adsorbed oxygen originating from NO. These oxygen atoms occupy active Pt sites for NO decomposition. Such an inhibiting
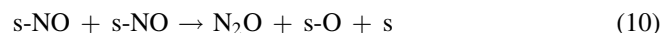
effect of oxygen species on NO decomposition under transient conditions has been already described for Pt/ZSM-5 [19] and Pt/Al₂O₃ [20].

The reaction pathway of N_2 formation during NO decomposition is usually ascribed to irreversible recombination of two adsorbed nitrogen atoms formed by NO dissociation [27–30]. However, no consensus was reached for the reaction pathways of N_2O formation. Two different reaction pathways have been discussed (Eqs. (9) and (10)):

- interaction between adsorbed NO and adsorbed N atom [19,20,31]:

$$s\text{-}NO + s\text{-}N \rightarrow N_2O + 2s \tag{9}$$

- interaction between two adsorbed NO [32,33]:

$$s\text{-}NO + s\text{-}NO \rightarrow N_2O + s\text{-}O + s \tag{10}$$

The participation of adsorbed nitrogen atoms in N_2O formation (Eq. (9) (also see Section 1)) was considered for Pt–Rh(1 0 0) alloy [31], Pt/ZSM-5 [19] and Pt/Al₂O₃ [20]. Additionally, this reaction pathway was essential for the description of oscillations of NO reduction with NH_3 over Pt(1 0 0) [34]. Recombination of two adsorbed NO species is commonly accepted to be the only reaction pathway of N_2O formation over Ag and Cu catalysts [35]. According to the tendency of different metal surfaces to dissociate NO depending on the position of the substrate in the periodic table [35], the same reaction pathway can be expected also for Pt. Burch et al. [36,37] have concluded from switch experiments between ^{14}NO and ^{15}NO, that N_2O formation over Pt/SiO₂ occurs via recombination of weakly bound NO molecules. Actually, density-functional calculations (DFT) performed for Pt(1 1 1) and Pt(2 1 1) predicted N_2O formation via the (NO)₂ intermediates over stepped Pt(2 1 1) surfaces [38]. The decisive evidence of the recombination of adsorbed NO molecules would be the detection of (NO)₂ species on the Pt surfaces, as reported for Ag, which is, however, still missing. Hence, both reaction pathways for N_2O formation should be considered in the following discussion of the interactions of ^{15}NO and $^{14}NH_3$.

4.2. Primary reaction steps of NH_3 and NO interaction

The importance of oxygen species for the ammonia activation has been stressed in recent investigations [18,22,26]. Considering these results it may be derived that the initial steps of NH_3 interaction with NO under conditions studied cannot be ascribed to ammonia dissociation, as predicted by previous mechanistic concepts [3–7,9–12]. Therefore, also for the reduction of NO with NH_3, the stripping of hydrogen atoms from the NH_3 molecule by oxygen species should be the dominating primary reaction step in the activation of ammonia under transient conditions. Oxygen species required for these stripping reactions were accumulated during oxygen treatment as was shown in Ref. [26] or they were supplied by NO decomposition.

4.3. Formation of N_2 in the interaction between $^{14}NH_3$ and ^{15}NO

The results of sequential pulsing of $^{14}NH_3$ and ^{15}NO (Fig. 7) indicate two different reaction steps for N_2 formation: (i) the "individual" reaction pathway of $^{15}N^{14}N$ formation, (ii) the "common" reaction pathway leading to the formation of $^{15}N_2$, $^{15}N^{14}N$ and $^{14}N_2$. From the distribution of differently labelled nitrogen molecules in the ^{15}NO pulses between 1 and 4 s it was concluded that the formation of various nitrogen isotopes occurred via recombination of nitrogen atoms. However, about half of the total amount of $^{15}N^{14}N$ should be ascribed to an individual reaction pathway taking into account that the rate of nitrogen formation is second order with respect to coverage by nitrogen atoms ($r = k_i \cdot \Theta_{s-N} \cdot \Theta_{s-N}$). Hereby, the formation of the same amounts of $^{15}N_2$, $^{15}N^{14}N$ and $^{14}N_2$ via recombination of ^{14}N and ^{15}N is predicted assuming equal coverage by adsorbed ^{15}N and ^{14}N species. If the coverage by one of the labelled nitrogen atoms will dominate over other, the formation of the respective nitrogen molecule is expected. Therefore, the dominant formation of $^{15}N^{14}N$ cannot be explained by recombination of differently labelled adsorbed nitrogen atoms only. Previously, $^{15}N^{14}N$ has been also observed as the main isotopically labelled nitrogen molecule in the reaction between $^{15}NH_3$ and ^{14}NO over an alumina-supported Pt catalyst [14] and a Pt(1 0 0) single crystal [6]. Otto et al. [14] have ascribed a possible "individual" pathway of $^{15}N^{14}N$ formation to the interaction between adsorbed $^{15}NH_2$ and NO species. This interaction can occur via surface intermediates like H_2NNO, suggested for non-catalytic, thermal reduction of NO with NH_3. These intermediates are characterised by a strong bond between nitrogen atoms, which remains during their rearrangement and decomposition to N_2 and H_2O [39]. However, the identification of ammonia fragments, which participate in this reaction, would require further spectroscopic studies supplemented by DFT calculations.

The interruption of nitrogen formation (Fig. 7) is explained by the inhibiting effect of NO. Such an inhibiting effect of NO on the reaction between NO and NH_3 was already observed over Pt wires, where NH_3–NO interactions were studied in NO excess [9]. Since NO does not completely desorb from polycrystalline Pt at 473 K [25,40], NO species, which occupy the active sites, hinder surface diffusion of nitrogen atoms and, hence, their recombination. Additionally, adsorbed NO species can suppress formation of oxygen species via NO dissociation [11] or hinder the surface diffusion of these oxygen species. As shown in [26], oxygen species initiate NH_3 dehydrogenation to adsorbed nitrogen atoms. If this reaction is inhibited, nitrogen atoms are not formed and, therefore, nitrogen formation is interrupted. As seen from Fig. 7 the formation of nitrogen via recombination of nitrogen atoms (between 1 and 4 s) starts during continuous desorption of ^{15}NO after most of the labelled nitric oxygen has already left the surface.

Desorption of nitric oxide is accelerated by an increase in temperature, therefore, the inhibiting effect of adsorbed ^{15}NO species on ^{15}NO decomposition decreases. The increasing amount of adso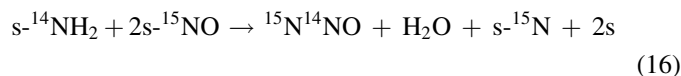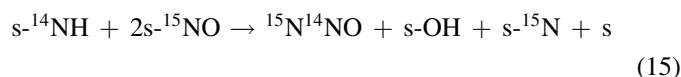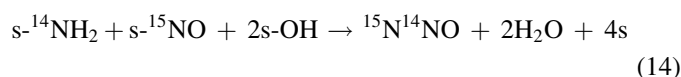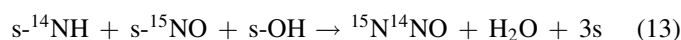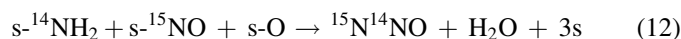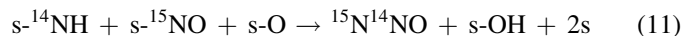rbed oxygen atoms formed via ^{15}NO dissocia-tion leads to an increase of H_2O formation by stepwise stripping of hydrogen atoms from ammonia molecules within the time range of the $^{14}NH_3$ pulses. Formed $^{14}NH_x$ species are consumed in the subsequent ^{15}NO pulse. Such a scenario explains the increase of H_2O formation at low temperatures in the $^{14}NH_3$ pulse and the prevalence of $^{15}N^{14}N$ in the subsequent ^{15}NO pulse (Fig. 5). Further temperature-dependent acceleration of ammonia oxidation in the NH_3 pulse leads to a decrease of the amount of ammonia fragments required for $^{15}N^{14}N$ formation in the subsequent ^{15}NO pulse. Thus, the changes in the molar fractions of $^{15}N_2$, $^{15}N^{14}N$ and $^{14}N_2$ occur mainly in accordance with the direct decomposition of ammonia and nitric oxide in the $^{14}NH_3$ and ^{15}NO pulses, respectively.

Summarising the results of sequential pulsing of NH_3 and NO, two reaction steps leading to formation of N_2 were confirmed, i.e. (i) the recombination of nitrogen atoms formed due to dissociation of NO and complete dehydrogenation of ammonia, (ii) interaction between adsorbed NO and ammonia fragments. The contribution of these reaction pathways to N_2 formation depends strongly on the relative coverage by adsorbed NO and NH_3.

4.4. Formation of N_2O in the interaction between $^{14}NH_3$ and ^{15}NO

Besides formation of N_2O due to NO decomposition, formation of differently labelled N_2O molecules at 473 K occurs between 0.2 and 0.7 s in the ^{15}NO pulse as shown in Fig. 9 upon sequential pulsing of $^{14}NH_3$ and ^{15}NO. In contrast to nitrogen formation, no formation of nitrous oxide was detected between 1 and 4 s at 473 K, although adsorbed nitrogen atoms being active in N_2 formation and adsorbed ^{15}NO species were still present on the surface (Fig. 7). These observations indicate that under conditions studied it is unlikely that nitrogen atoms participate in the formation of N_2O. With respect to the alternative reaction pathways suggested in literature [3,9,10,14] the formation of differently labelled N_2O molecules can occur via either recombination of adsorbed NO molecules or via interaction between NO and ammonia fragments. The recombination of adsorbed NO molecules alone cannot, however, explain the absence of $^{14}N_2O$ at 473 K. This statement is based on the fact that $^{15}N^{14}NO$ is formed at higher concentration than $^{15}N^{15}NO$ (Fig. 6). Therefore, high concentration of adsorbed ^{14}NO species would be expected if nitrous oxide is formed via the recombination of adsorbed NO molecules. However, $^{14}N_2O$ was not detected. Also the coupling between adsorbed NO molecules and ammonia fragments is not appropriate as the only reaction pathway of N_2O, since it requires the formation of $^{15}NH_x$ under excess of NO on the surface. Therefore, in agreement with Otto et al. [14] an individual pathway of $^{15}N^{14}NO$ via coupling between adsorbed NH_x and NO species has to be considered. This reaction pathway suggested the formation of adsorbed hydrogen atoms, which can also recombine yielding H_2. However, gas-phase H_2 was never observed in the ^{15}NO pulse in the present experiments in spite of the applied pressure conditions, which would favour its desorption. The discrepancy between the suggested reaction pathway of N_2O formation via NH_2–NO

coupling [14] and the present experimental observations can be overcome by assuming participation of additional oxygen-containing species, which react with hydrogen atoms of the NH_x ($x = 1, 2$) fragments. Such oxygen species can be oxygen atoms (Eqs. (11) and (12)) OH groups (Eqs. (13) and (14)) or another NO molecule (Eqs. (15) and (16)):

$$s\text{-}^{14}NH + s\text{-}^{15}NO + s\text{-}O \rightarrow {}^{15}N^{14}NO + s\text{-}OH + 2s \quad (11)$$

$$s\text{-}^{14}NH_2 + s\text{-}^{15}NO + s\text{-}O \rightarrow {}^{15}N^{14}NO + H_2O + 3s \quad (12)$$

$$s\text{-}^{14}NH + s\text{-}^{15}NO + s\text{-}OH \rightarrow {}^{15}N^{14}NO + H_2O + 3s \quad (13)$$

$$s\text{-}^{14}NH_2 + s\text{-}^{15}NO + 2s\text{-}OH \rightarrow {}^{15}N^{14}NO + 2H_2O + 4s \quad (14)$$

$$s\text{-}^{14}NH + 2s\text{-}^{15}NO \rightarrow {}^{15}N^{14}NO + s\text{-}OH + s\text{-}^{15}N + s \quad (15)$$

$$s\text{-}^{14}NH_2 + 2s\text{-}^{15}NO \rightarrow {}^{15}N^{14}NO + H_2O + s\text{-}^{15}N + 2s \quad (16)$$

However, no information on the nature of these oxygen-containing species could be derived in the present study. This aspect of the interaction between NO and NH_3 as well as the structure of the reaction intermediate needs still further investigations.

The formation of $^{15}N_2O$ was in turn ascribed to the recombination of two adsorbed NO molecules. In coincidence with findings of Burch et al. [36,37] this assumption explains the formation of N_2O during NO decomposition over hydrogen-treated Pt gauze at 473 K, where no N_2 formation was detected. The contribution of this reaction pathway to the overall formation of N_2O in NO reduction by NH_3 depends strongly on the coverage by NO species, since it is a second-order reaction. Above 973 no formation of N_2O via recombination of two adsorbed NO molecules should take place, since this reaction is thermodynamically forbidden at these temperatures [1]. Therefore, as it was mentioned in Ref. [8] the interaction between nitric oxide and ammonia fragments is the only reaction pathway of N_2O formation above 973 K.

5. Conclusions

Specific mechanistic conclusions for N_2 and N_2O formation were derived from the results of single ^{14}NO and sequential $^{14}NH_3$ and ^{15}NO pulsing over polycrystalline Pt catalyst in the temperature range from 323 to 973 K for peak pressure of ca. 10 Pa.

N_2 formation was established to occur via two reaction pathways: (i) *interaction between adsorbed NO and NH_x species* and (ii) *recombination of two adsorbed nitrogen atoms*, which originated from NO dissociation or/and complete NH_3 dehydrogenation. The recombination of adsorbed nitrogen atoms is hindered by adsorbed NO species below 573 K. For N_2O formation two independent reaction pathways were identified: (i) *recombination of two NO molecules* and (ii) *interaction between adsorbed NH_x and NO*, which probably

requires participation of additional oxygen-containing species. The contribution of the above reactions to total product formation depends strongly on the coverage of the catalyst surface by adsorbed NH_x and NO species and on the reaction temperature. The suggested reaction steps of product formation in the interaction between NO and NH_3 certainly offer a better understanding the performance of real catalytic system on a fundamental level.

Acknowledgements

References

[1] V.I. Parvulescu, P. Grange, B. Delmon, Catal. Today 46 (1998) 233.
[2] H.C. Andersen, W.J. Green, D.R. Steele, Ind. Eng. Chem. 53 (1988) 199.
[3] C.G. Takoudis, L.D. Schmidt, J. Phys. Chem. 87 (1983) 964.
[4] P. Nowobilski, C.G. Takoudis, Chem. Eng. Sci. 40 (1985) 1751.
[5] S.J. Lombardo, M. Slinko, T. Fink, T. Löher, H.H. Madden, F. Esch, R. Imbihl, Surf. Sci. 269–270 (1992) 481.
[6] S.J. Lombardo, F. Esch, R. Imbihl, Surf. Sci. Lett. 271 (1992) L367.
[7] M.F.H. van Tol, J. Siera, P.D. Cobden, B.E. Nieuwenhuys, Surf. Sci. 274 (1992) 63.
[8] J. Pérez-Ramírez, E.V. Kondratenko, V.A. Kondratenko, M. Baerns, J. Catal. 229 (2005) 303.
[9] J.L. Gland, V.N. Korchak, J. Catal. 55 (1978) 324.
[10] C.G. Takoudis, L.D. Schmidt, J. Phys. Chem. 87 (1983) 958.
[11] T. Katona, L. Guczi, G.A. Somorjai, J. Catal. 132 (1991) 440.
[12] T. Katona, L. Guczi, G.A. Somorjai, J. Catal. 135 (1992) 434.
[13] J.L. Gland, V.N. Korchak, J. Catal. 53 (1978) 9.
[14] K. Otto, M. Shelef, J.T. Kummer, J. Phys. Chem. 74 (1970) 2690.
[15] M.Y. Smirnov, V.V. Gorodetskii, J.H. Block, J. Mol. Catal. A: Chem. 107 (1996) 359.
[16] W.D. Mieher, W. Ho, Surf. Sci. 322 (1995) 151.
[17] A.C.M. van den Broek, J. van Grondelle, R.A. van Santen, J. Catal. 185 (1999) 297.
[18] D.P. Sobczyk, A.M. de Jong, E.J.M. Hensen, R.A. van Santen, J. Catal. 219 (2003) 156.
[19] C. Rottländer, R. Andorf, C. Plog, B. Krutzsch, M. Baerns, J. Catal. 169 (1997) 400.
[20] A.R. Vaccaro, G. Mul, J.A. Moulijn, in: G.F. Froment, K.C. Waugh (Eds.), Reaction Kinetics and the Development and Operation of Catalytic Processes, Elsiever Science B.V, 2001, p. 357.
[21] R.J. Mukerji, A.S. Bolina, W.A. Brown, Surf. Sci. 547 (2003) 27.
[22] J. Pérez-Ramírez, E.V. Kondratenko, V.A. Kondratenko, M. Baerns, J. Catal. 227 (2004) 90.
[23] J.T. Gleaves, J.R. Ebner, T.C. Kuechler, Catal. Rev. Sci. Eng. 30 (1988) 49.
[24] J.T. Gleaves, G.S. Yablonsky, P. Phanawadee, Y. Schuurman, Appl. Catal. A: Gen. 160 (1997) 55.
[25] C.L. Levoguer, R.M. Nix, Surf. Sci. 365 (1996) 672.
[26] M. Baerns, R. Imbihl, V.A. Kondratenko, R. Kraehnert, W.K. Offermans, R.A. van Santen, A. Scheibe, J. Catal. 232 (2005) 226.
[27] E.D.L. Rienks, J.W. Bakker, A. Baraldi, S.A.C. Carabineiro, S. Lizzit, C.J. Weststrate, B.E. Nieuwenhuys, Surf. Sci. 516 (2002) 109.
[28] D.Y. Zemlyanov, M.Y. Smirnov, V.V. Gorodetskii, J.H. Block, Surf. Sci. 329 (1995) 61.
[29] A. Bogicevic, K.C. Hass, Surf. Sci. 506 (2002) L237.

[30] A. Eichler, J. Hafner, Chem. Phys. Lett. 343 (2001) 383.

[31] H. Hirano, T. Yamada, K.I. Tanaka, J. Siera, P. Cobden, B.E. Nieuwen-huys, Surf. Sci. 262 (1993) 97.

[32] P. Denton, Y. Schuurman, A. Giroir-Fendler, H. Praliaud, M. Primet, C. Mirodatos, Chemistry 3 (2000) 437.

[33] H. Ibach, S. Lehwald, Surf. Sci. 76 (1978) 1.

[34] A.V. Walker, M. Gruyters, D.A. King, Surf. Sci. 384 (1997) L791.

[35] W.A. Brown, D.A. King, J. Phys. Chem. B 104 (2000) 2578.

[36] R. Burch, A.A. Shestov, J.A. Sullivan, J. Catal. 186 (1999) 353.

[37] R. Burch, A.A. Shestov, J.A. Sullivan, J. Catal. 188 (1999) 69.

[38] R. Burch, S.T. Daniells, P. Hu, J. Chem. Phys. 121 (2004) 2737.

[39] D. Fang, L.B. Harding, S.J. Klippenstein, J.A. Miller, Faraday Discuss. 119 (2001) 207.

[40] M.J. Mummey, L.D. Schmidt, Surf. Sci. 109 (1981) 43.